Synthesis, characterization, luminescence, antibacterial, and catalytic activities of a palladium(II) complex involving a Schiff base

De-Yun Ma [a] [b] , Le-Xin Zhang [a] , Xuan-Ye Rao [a] , Tong-Liang Wu [a] , Dong-Hao Li [a] & Xiao-Qun Xie [a]

[a] School of Chemistry and Chemical Engineering , Zhaoqing University , Zhaoqing , P.R. China

[b] The Key Laboratory of Fuel Cell Technology of Guangdong Province , South China University of Technology , Guangzhou , P.R. China
Accepted author version posted online: 12 Mar 2013.Published online: 16 Apr 2013.

PLEASE SCROLL DOWN FOR ARTICLE

Taylor & Francis
Taylor & Francis Group

Synthesis, characterization, luminescence, antibacterial, and catalytic activities of a palladium(II) complex involving a Schiff base

DE-YUN MA*†‡, LE-XIN ZHANG†, XUAN-YE RAO†, TONG-LIANG WU†, DONG-HAO LI† and XIAO-QUN XIE†

†School of Chemistry and Chemical Engineering, Zhaoqing University, Zhaoqing, P.R. China
‡The Key Laboratory of Fuel Cell Technology of Guangdong Province, South China University of Technology, Guangzhou, P.R. China

A new Pd(II) complex of fluorine-containing Schiff base ligand, $[Pd_2(L)_2Cl_2]$ (**1**) [**L** = N-(4-fluorobenzylidene)-2,6-diethylbenzenamine], has been synthesized using solvothermal method and characterized by elemental analysis, IR-spectroscopy, thermogravimetric analysis, powder X-ray diffraction, UV–vis absorption spectra, and single-crystal X-ray diffraction. Complex **1** is a μ-chloro-bridged dinuclear cyclometallated Pd(II) complex. Thermal analysis indicates that **1** is quite stable to heat. **1** exhibits quadruple emissions in the solid state ($\lambda_{max} = 766$ nm) and possesses fluorescence lifetimes ($\tau_1 = 87.20$ ns, $\tau_2 = 190.45$ ns, and $\tau_3 = 1805.10$ ns at 616 nm); broad structureless bands at 690–800 nm are tentatively assigned to an excimeric ^3IL transition. The Schiff base (**L**) and its palladium(II) compound (**1**) have been screened for their antibacterial activity against several bacteria, and the results are compared with the activity of penicillin. Moreover, **1** has been shown to be highly effective in the Heck reaction of 4-bromotoluene with acrylic acid.

Keywords: Schiff base; Palladium(II) complex; Luminescent; Antibacterial activity; Catalytic activity

1. Introduction

Schiff bases have a wide range of biological activities and industrial applications [1]. Palladium(II) complexes based on Schiff bases have gained increasing recognition due to potential applications in luminescence, catalysis, and bacteriostasis [2–5]. Photophysics and photoreactivity of coordinatively unsaturated platinum(II) complexes and their applications as luminescent sensors are of considerable interest in inorganic photochemistry [6,7]. Compared to platinum(II) complexes, little attention has been focused on luminescent characteristics of palladium(II) complexes [2]. Fluorine-containing Schiff bases have superior biological activity compared to Schiff bases without fluorine [8]. Numerous drugs

---

*Corresponding author. Email: mady@zqu.edu.cn

containing fluorine, including antipsychotics such as fluphenazine, HIV protease inhibitors such as fipranavir, antibiotics such as oflaxacin and trovafloxacin, and anasthetics such as halothae have been reported [9,10]. Arylation and alkenylation of alkenes with a palladium catalyst (the Heck reaction) [11] have become mainstays of modern synthetic organic chemistry for the formation of carbon–carbon bonds. Compared to homogeneous catalysis for such coupling reactions, heterogeneous catalysis involving supported metal complexes offers several advantages, such as robustness and increased air and moisture stability [12,13]. Palladium(II) complexes derived from Schiff base ligands have been extensively studied over the past few decades for applications as heterogeneous catalysts in organic reactions [4]. On the basis of the above considerations, we report the synthesis, characterization, and properties of a new Pd(II) complex based on a fluorine-containing Schiff base.

2. Experimental

2.1. *Materials and physical measurements*

All chemicals were commercially available and used as received without purification. Elemental analyses for C, H, and N were carried out using a Vario EL III Elemental Analyzer. Infrared spectra were recorded (4000–400 cm^{-1}) as KBr disks on a Shimadzu IR-440 spectrometer. Thermogravimetric analyses (TGA) were performed on an automatic simultaneous thermal analyzer (DTG-60, Shimadzu) under a flow of N_2 at a heating rate of 10 °C min^{-1} between ambient temperature and 800 °C. Powder XRD investigations were carried out on a Bruker AXS D8-Advanced diffractometer at 40 kV and 40 mA with Cu-Kα ($\lambda = 1.5406$ Å) radiation. UV–vis absorption spectra were measured using a Shimadzu UV-160A spectrophotometer. Luminescence spectra and lifetimes for crystalline samples were recorded at room temperature on an Edinburgh FLS920 phosphorimeter. Nuclear Magnetic Resonance spectra were recorded on a Bruker Avance 400 MHz spectrometer. ^{1}H NMR chemical shifts are reported in ppm from tetramethylsilane with the solvent resonance as the internal standard (CDCl$_3$, $\delta = 7.26$). Data are reported as follows: chemical shift (δ ppm), multiplicity, coupling constants (Hz), integration, and assignment. ^{13}C NMR spectra were collected on a 100 MHz spectrometer with complete proton decoupling. Chemical shifts are reported in ppm from tetramethylsilane with the solvent resonance as internal standard (CDCl$_3$, $\delta = 77.23$). Melting points were measured uncorrected with a Mel-Temp apparatus.

2.2. *Solvothermal synthesis*

2.2.1. Preparation of L.   L was prepared by the condensation of 4-fluorobenzaldehyde (2.48 g, 20 mmol) with 2,6-diethylaniline (2.98 g, 20 mmol) in ethanol (20 mL) as the reaction medium. The solution was refluxed for 4 h and then allowed to cool to room temperature. The yellow precipitate was recrystallized from ethanol to give **L** as straw-yellow crystals. Yield 3.25 g (66%). ^{1}H NMR (400 MHz, CDCl$_3$) δ: 8.18 (s, 1H, C**H**N), 7.04–7.92 (m, 6H, Ar–H), 2.49 [q, $J = 5.0$ Hz, 4H, C**H$_2$**CH$_3$], 1.13 (t, $J = 0.28$ Hz, 6H, CH$_3$); ^{13}C NMR (100 MHz, CDCl$_3$) δ: 165.7, 164.0, 160.6, 150.2, 133.1, 132.4, 132.4, 130.5, 130.4, 126.3, 124.0, 116.0, 115.9, 24.7, 14.6; MP: 62–64 °C. Anal. for C$_{16}$H$_{18}$NF (%): Calcd C, 78.0; H, 7.3; N, 5.7. Found: C, 78.5; H, 7.1; N, 5.4. FTIR (KBr, cm^{-1}):

2974(m), 2876(w), 1645(s), 1593(s), 1508(s), 1456(m), 1417(w), 1375(w), 1292(w), 1234 (s), 1178(m), 1153(m), 1093(m), 1062(w), 1008(w), 883(s), 837(s), 794(m), 746(s), 690 (w), 619(w), 561(w), 524(w), 493(w), 441(w).

2.2.2. Preparation of [Pd$_2$(L)$_2$Cl$_2$] (1). Na$_2$PdCl$_4$ (0.0887 g, 0.5 mmol) was dissolved in methanol (10 mL). **L** (0.246 g, 1 mmol) was added and the mixture stirred at room temperature for 5 h under an inert atmosphere. The resulting mixture was filtered under reduced pressure. The collected solid was washed with ethyl ether and dried in air to give yellow crystals that were purified by recrystallization from methylene chloride (15 mL) and hexane (10 mL). Yield 0.171 g (86%). Anal. for C$_{34}$H$_{34}$N$_2$Cl$_2$F$_2$Pd$_2$ (%): Calcd C, 51.5; H, 4.3; N, 3.5. Found: C, 51.9; H, 4.0; N, 3.3. FTIR (KBr, cm^{-1}): 3467(s), 2970(m), 2877(w), 1608 (vs), 1582(m), 1562(s), 1460(s), 1406(w), 1348(w), 1296(m), 1249(m), 1226(m), 1182(m), 1027(m), 973(w), 918(w), 868(s), 814(s), 765(m), 669(w), 582(w), 455(w), 414(w).

2.3. *Antibacterial activity tests*

In vitro bacterial activities of the Schiff base and its palladium(II) complex were tested using the paper disk diffusion method. The chosen strains were G(+)*Staphylococcus aureus* and *Bacillus cereus* and *Rhizopus* and *Escherichia coli*. The liquid medium containing the bacterial subcultures was autoclaved for 20 min at 15 lb pressure before inoculation. The bacteria were cultured for 24 h at 35 °C in an incubator. Mueller-Hinton broth was used for preparing basal media for the bioassay of the organisms. Nutrient agar was poured onto a Petri plate and allowed to solidify. The test compounds were dissolved in dimethylformamide (DMF) and were added dropwise to 10 mm diameter paper disks placed in the center of the agar plates. The plates were then kept at 5 °C for 1 h and transferred to an incubator maintained at 35 °C. The width of the growth inhibition zone around the disk was measured after 24 h of incubation. Four replicates were taken for each treatment. In order to clarify any role of DMF in the biological screening, separate studies are carried out with solutions of DMF alone and they show no activity against any bacterial strains.

2.4. *Catalytic reactions*

A mixture of 4-bromotoluene (1.0 mmol), acrylic acid (1.3 mmol), triethylamine (2.0 mmol), DMF (6 mL), and 0.5 mol% of catalyst was stirred at 80 °C under air. After the reaction, the catalyst was separated by filtration. The filtrate was dried over Na$_2$SO$_4$ and filtered. The products were quantified by Gas Chromatography and Mass Spectrometry (GC–MS) analysis (Shimadzu GCMS-QP5050A equipped with a 0.25 mm × 30 m DB-WAX capillary column). The typical GC–MS analysis program was as follows: initial column temperature 100 °C, hold 2 min, ramp temperature to 280 °C at 15 °C min^{-1}, and hold for 5 min.

Table 1.   Crystallographic data of **1**.

Empirical formula	$C_{38}H_{42}N_2Cl_2F_2Pd_2$
Formula weight	848.44
Temperature (K)	296(2)
Size (mm)	$0.30 \times 0.27 \times 0.22$
Crystal system	Monoclinic
Space group	$P2_1/c$
a (Å)	11.2951(12)
b (Å)	10.3255(11)
c (Å)	16.9093(17)
β (°)	105.552(2)
V (Å^3)	1899.9(3)
Z	2
D (Mg m^3)	1.483
Limiting indices	$-13 \leqslant h \leqslant 11, -12 \leqslant k \leqslant 12, -20 \leqslant l \leqslant 19$
Reflections collected/unique	10,171/3399
R_{int}	0.0242
$F(000)$	856
θ (°)	2.72–25.20
Goodness-of-fit on F^2	1.085
$R(I> 2\sigma)$	$R_1 = 0.0286$ $wR_2 = 0.0903$
R (all data)	$R_1 = 0.0411$ $wR_2 = 0.1178$
Largest diff. peak and hole (Å^{-3})	0.99, -1.25

Notes: $R = \sum(||F_o| - |F_c||)/\sum|F_o|$.
$wR = [\sum w(F_o^2 - F_c^2)^2/\sum w(F_o^2)^2]^{1/2}$.

2.5. *X-ray crystallography*

Single-crystal X-ray diffraction analysis of **1** was performed on a Bruker Apex II CCD diffractometer operating at 50 kV and 30 mA using MoKα radiation ($\lambda = 0.71073$ Å). Data collection and reduction were performed using APEX II software [14]. Multi-scan absorption corrections were applied for all the data-sets using SADABS, as included in the APEX II program [14]. Small residual absorption effects were treated with XABS2 [15]. The structure was solved by direct methods and refined by least squares on F^2 using the SHELXTL program package [16]. All non-hydrogen atoms were refined with anisotropic

Table 2.   Selected bond distances (Å) and angles (°) for **1**.

Pd1–N1	2.024(4)	Pd1–C13	1.972(5)
Pd1–Cl1	2.3307(13)	Pd1–Cl1^i	2.4531(13)
C13–Pd1–N1	81.2(2)	C13–Pd1–Cl1	95.97(18)
N1–Pd1–Cl1	173.98(14)	C13–Pd1–Cl1^i	177.19(17)
N1–Pd1–Cl1^i	96.57(13)	Cl1–Pd1–Cl1^i	86.39(5)

Note: Symmetry code: i $-x$, y, $0.5-z$.

Table 3.   Hydrogen bond geometries for **1** (Å, °).

D–H···A	d(D–H)	d(H···A)	d(D···A)	<D–H···A
C17–H17···Cl1	0.93	2.79	3.523(2)	137
C7–H7A···N1^i	0.97	2.36	2.838(1)	110
C9–H9A···N1	0.97	2.49	2.879(6)	104
C14–H14···Cl1	0.93	2.77	3.313(5)	118

displacement parameters. Hydrogens attached to carbon and oxygen were placed in geometrically idealized positions and refined using a riding model. Crystallographic data are listed in table 1. Selected bond lengths and angles, and H-bonding parameters for the compound are given in tables 2 and 3, respectively.

3. Results and discussion

3.1. *Structure of 1*

To prepare **1**, the Schiff base was treated with Na_2PdCl_4 in equimolar amounts at room temperature in methanol. The reactions proceeded without reflux under mild conditions.

The molecular structure of **1** is shown in figure 1. Selected bond distances and angles are given in table 2. In **1**, each **L** is bonded to the di-μ-chloro-bridged unit through nitrogen and an aromatic carbon, providing two equivalent five-membered N–C–Pd–C-chelate rings. The geometry at the Pd(II) center in **1** is almost square planar, with the two cyclo-metallated ligands in a *trans* arrangement with respect to the Pd···Pd axis. The Pd1–C13 bond [1.972(2) Å] is shorter than the expected value of 2.08 Å based on the sum of the covalent radii of carbon and palladium, but consistent with those found for related complexes where partial multiple-bond character of the Pd–C was assumed [17,18]. The Pd1–N1 bond distance [2.025(3) Å] is in agreement with the sum of covalent radii for nitrogen and palladium [19], and similar to the values reported previously [17,18]. The lengths of the Pd–Cl bonds *trans* to C [2.453(2) Å] and the Pd–Cl bonds *trans* to N [2.331 (4) Å] reflect the different *trans* influences exerted by the phenyl carbons and nitrogens. In
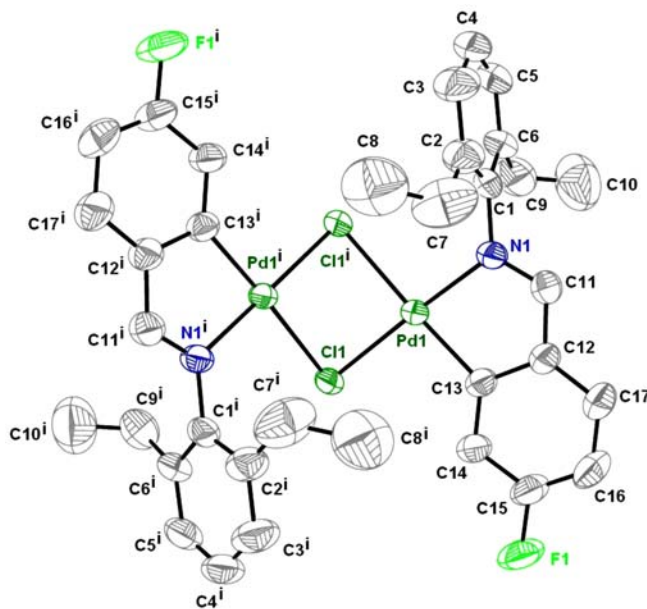

Figure 1. The molecular structure of **1** with numbering scheme (all hydrogens are omitted for clarity). Symmetry code: (i) −*x*, *y*, 0.5−*z*.
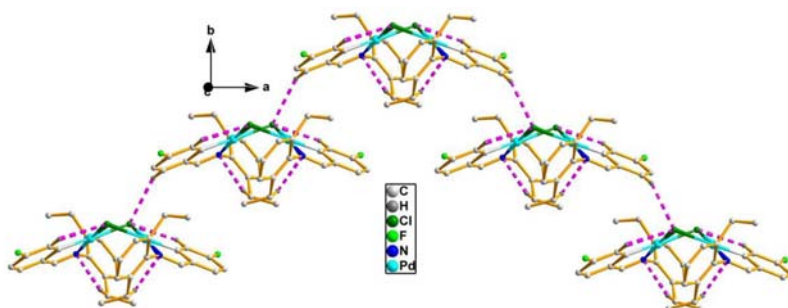
Figure 2. View of an arch-like chain formed by hydrogen-bonding interactions (pink dashes) (see http://dx.doi. org/10.1080/00206814.2013.783699 for color version).

the five-membered chelate rings, Pd1, N1, C11, C12, and C13 are essentially planar. The bite angle [C15–Pd1–N1 = 81.24(4)°] is in agreement with those found in a structurally related μ-Cl dimer [18]. The Pd_2Cl_2 ring is significantly folded with the angle between the two planes defined by Pd1, Cl1, Cl1^i and Pd1^i, Cl1, Cl1^i is 52.63, comparable to those found in similar complexes [20]. Pd1 and Pd1^i are linked by chlorides Cl1 and Cl1^i with a Pd1···Pd1^i separation of 3.12(8) Å, which, being shorter than the double van der Waals radius of Pd(II) (1.79 Å), indicates a weak Pd···Pd interaction (symmetry code: $i = -x$, y, $0.5-z$). In the crystal of **1**, an arch-like chain is formed through C17–H17···Cl1 hydrogen bonding interactions (figure 2). Moreover, intramolecular C–H···N and C–H···Cl hydrogen bonds are also observed (table 3).

3.2. *Powder X-ray diffraction analysis*

In order to check the purity of **1**, bulk samples were measured by X-ray powder diffraction at room temperature. As shown in Supplementary material, the peak positions of the experimental patterns are in agreement with the simulated patterns, which clearly indicate purity of the complexes.

3.3. *Infrared spectra and TGA*

FTIR spectra of **L** and **1** were recorded as KBr pellets (Supplementary material). In the IR spectrum, strong, broad bands at 3467 cm^{-1} for **1** may be assigned to v(O–H) stretch of water (impurity). Features at 2974, 2876, and 1645 cm^{-1} for **L**, 2970, 2877, and 1608 cm^{-1} for **1** are associated with the methyl, methylene, and –CH=N–, respectively.

The TG and DTA curves of **1** are shown in Supplementary material. Complex **1** has thermal stability as no clean weight loss step occurs below 220 °C. The weight loss above 220 °C corresponds to the decomposition of the framework structure.

3.4. *Electronic absorption and emission properties of L and 1*

Both **L** and **1** show low-energy absorptions at *ca.* 310–400 nm and higher energy bands at *ca.* 250–300 nm in DMF (figure 3). From 200 to 800 nm, the B band of **L**, which is attributed to the π–π* transition, is the most intense absorption at 252 nm. The second most
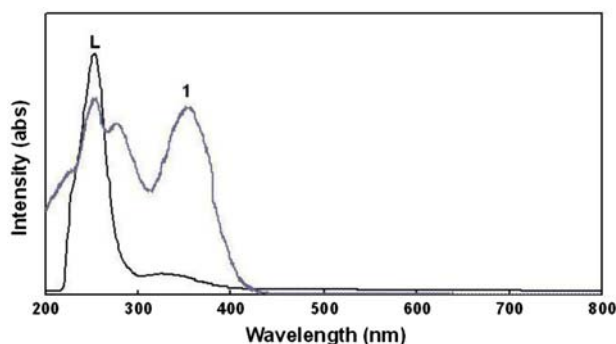
Figure 3.   UV–vis absorption spectra of **L** and **1** in DMF.

Table 4.   Photophysical data.

Compounds	Medium (T K^{-1})	λ nm^{-1} (e dm^{-3} mol^{-1} cm^{-1})	Emission λ nm^{-1}
Ligand **L**	DMF (298)	252 (34,800), 334 (14,700)	Non-tested
Complex **1**	DMF (298)	254 (36,000), 278 (21,200), 355 (12,900)	Non-emission
	Solid (298)	Non-tested	616, 697, 715, 766

intense absorption at 334 corresponds to the K band of the charge-transfer transition between benzene rings and –C=N–. The high energy absorption band is assigned as intraligand (IL) transitions of **1,** based on its similarity to that of free **L** (252 nm in DMF). The photophysical data for **L** and **1** are summarized in table 4. With reference to previous spectroscopic work on a series of *cis*- and *trans*-[M(PR$_3$)$_2$(X)(Y)] (M = Pd, Pt) [21–23], [Ni(PMe$_3$)$_3$X$_2$] [24], [Pd$_2$(P^P)$_2$X$_4$] [25], [Pd(dbcpe)X$_2$] [26], and the close analogy of palladium(II) compounds with platinum analogs and the nickel(II) congeners, the low-energy absorption at *ca.* 350–400 nm is tentatively assigned as a ligand-to-metal charge transfer [LMCT, p$_\pi$(X) → 4d(Pd)] transition in **1**.

As part of a continuing program dedicated to luminescent d^8 systems, the spectroscopic behavior of **1** is presented. Complex **1** is non-emissive in DMF at room temperature,
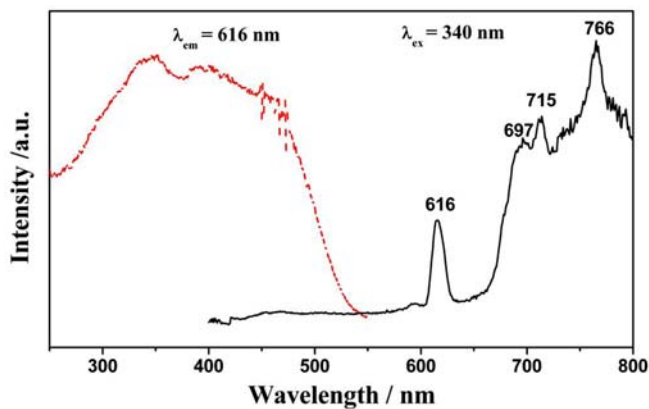

Figure 4.   Solid-state excitation and emission spectra of **1** at room temperature.
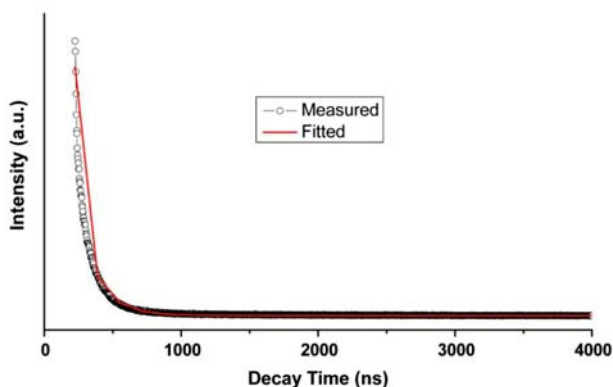
Figure 5.   Luminescent lifetimes for **1** in the solid-state at room temperature.

similar to previous references [2,3]. Solid-state emission luminescence spectra of **1** at room temperature are shown in figure 4. The emission spectrum shows sharp band at $\lambda_{max} = 616$ nm and three structureless bands at $\lambda_{max} = 697$, 715, and 766 nm. Both absorption and solid-state excitation spectra for **1** reveal low-energy ligand-field states in the 330–550 nm spectral region. The high-energy structured band of **1** is assigned to a transition to a ^{3}IL excited state [2]. The broad structureless emission at 690–800 nm is tentatively assigned to an excimeric ^{3}IL transition [2]. The luminescent lifetimes of **1** using an Edinburgh FLS S920 phosphorimeter with a 450 W xenon lamp as excitation source show lifetimes for **1** of $\tau_1 = 87.20$ ns, $\tau_2 = 190.45$ ns, and $\tau_3 = 1805.10$ ns at 616 nm (figure 5).

3.5. *Biological activity tests*

The susceptibility of certain strains of bacterium towards **L** and **1** were judged by measuring the size of bactericidal diameter. The results are given in table 5. The effect against *S. aureus* of **L** and **1** was very close to sodium penicillinate itself. Both **L** and **1** showed inhibition diameters larger than sodium penicillinate against *B. cereus*. Compared to **L** and **1**, which show good activities, penicillin is ineffective against *rhizopus* and

Table 5.   Antimicrobial activities of **L** and **1**.

Entry	(μg/disk)	Zone of inhibition (mm)			
		S. aureus	*B. cereus*	*Rhizopus*	*E. coli*
L	20	30.2	20.4	21.2	23.8
	10	27.8	18.7	19.4	22.1
	2	20.3	16.5	17.1	20.4
1	20	32.7	23.4	25.5	26.7
	10	31.9	21.7	23.1	24.5
	2	24.6	20.1	20.1	21.2
Penicillin	20	34.7	12.2	0.0	0.0
	10	14.8	0.0	0.0	0.0
	2	0.0	0.0	0.0	0.0
DMF	20	–	–	–	–
	10	–	–	–	–
	2	–	–	–	–

Table 6. The effect of base and solvent on **1** catalyzed Heck reaction of 4-bromotoluene with acrylic acid.
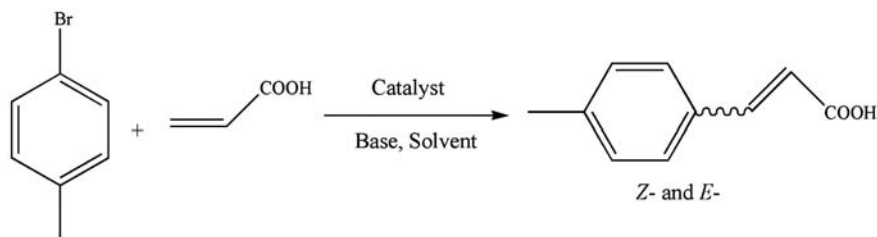
Entry	Base	Solvent	Temperature (°C)	Atmosphere	Time (h)	Yields (%)
1	Et_3N	DMF	80	Air	5	92
2	Et_3N	DMF	50	Air	5	86
3	Et_3N	DMF	120	Air	5	83
4	Et_3N	Methanol	80	Air	5	65
5	Et_3N	ACN	80	Air	5	51
6	Et_3N	Toluene	80	Air	5	32
7	Na_3PO_4	DMF	80	Air	5	45
8	K_2CO_3	DMF	80	Air	5	41
9	Na_2CO_3	DMF	80	Air		34
10	NaOAc	DMF	80	Air	5	22
11	KF	DMF	80	Air	5	–

E. coli. Moreover, we found that **1** shows superior activity to **L**. It is possible that **L** may be activated by Pd^{2+} [27]. Compared to those palladium(II) complexes, which the ligands excluding fluorine, **L** and **1** show superior biological activity [28–32]. For example, Carvalho *et al.* reported a palladium(II) complex with the amino acid L-tryptophan (Pd-TRP), which exhibited inhibition zones for *E. coli* and *S. aureus* of 13.0 and 12.0 mm under 800 μg compounds, being comparable to the 26.7 and 32.7 mm under 200 μg of **1** [28]. El-Sherif also reported a series of palladium complexes and they show antibacterial activities against *Streptococcus pyogenes* and *E. coli* bacteria at different concentrations 1, 2.5, and 5 mg mL^{-1} in DMSO, which the activities are much smaller than **1** and **L** [29]. The results obtained for **1** and **L** show better antibacterial activities to platinum(II) and palladium(II) complexes based on Schiff bases [33].

3.6. *Heck reaction catalysis*

Base and solvent for the Heck reaction greatly influence catalytic activity (table 6); reaction temperature has less effect on the catalytic activity. DMF is the best solvent for this catalytic system. In other organic solvents, e.g. methanol, acetonitrile, or toluene, relatively low yields of coupling products were obtained. Among six different bases investigated for these reactions, Et_3N was most effective (table 6, entry 1); Na_3PO_4, NaOAc, K_2CO_3, and Na_2CO_3 were substantially less effective. KF failed to promote the reaction (table 6, entry 11). Compared to other Pd(II) complexes containing Schiff bases, the catalytic activities of the present complex for the Heck reaction proved to be highly effective [13].

4. Conclusion

We have described the synthesis of a new fluorine-containing Schiff base and its Pd(II) complex. Complex **1** shows good thermal stability and exhibits photoluminescence in the solid-state at room temperature (616, 697, 715 and 766 nm) with lifetimes of $\tau_1 = 87.20$ ns, $\tau_2 = 190.45$ ns, and $\tau_3 = 1805.10$ ns at 616 nm. Antibacterial activity tests show that **L** and **1** exhibit superior biological activity against *S. aureus*, *B. cereus*, *rhizopus,* and *E. coli*. Complex **1** exhibits high catalytic activity in the Heck coupling reaction of 4-bromotoluene with acrylic acid, which is very sensitive to the choice of base and solvent.

Supplementary material

Crystallographic data for the structural analysis has been deposited with the Cambridge Crystallographic Data Center; CCDC reference number is 907218. Copies of this information may be obtained free of charge on application to CCDC, 12 Union Road, Cambridge CB2 1EZ, UK (Fax: +44-1223-336-033; E-mail: deposit@ccdc.cam.ac.uk or www: http://www.ccdc.cam.ac.uk). The additional figures can be obtained from the web free of cost.

Acknowledgements

References

[1] S. Kumar, M.S. Niranjan, K.C. Chaluvaraju, C.M. Jamakhandi, D.J. Kadadevar. *J. Curr. Pharm. Res.*, **01**, 39 (2010).
[2] S.W. Lai, T.C. Cheung, M.C.W. Chan, K.K. Cheung, S.M. Peng, C.M. Che. *Inorg. Chem.*, **39**, 255 (2000).
[3] B.C. Tzeng, S.C. Chan, M.C.W. Chan, C.M. Che, K.K. Cheung, S.M. Peng. *Inorg. Chem.*, **40**, 6699 (2001).
[4] V.K. Jain, L. Jain. *Coord. Chem. Rev.*, **249**, 3075 (2005).
[5] J.R. Anacona, E. Bastardo. *Transition Met. Chem.*, **24**, 478 (1999).
[6] S.D. Cummings, R. Eisenberg. *J. Am. Chem. Soc.*, **118**, 1949 (1996).
[7] K.H. Wong, M.C.W. Chan, C.M. Che. *Chem. Eur. J.*, **5**, 2845 (1999).
[8] H. Sawada, K. Yanagida, Y. Inaba, M. Sugiya, T. Kawase, T. Tomita. *Eur. Polym. J.*, **37**, 1433 (2001).
[9] M.S. Karthikeyan, B.S. Holla, N.S. Kumari. *Eur. J. Med. Chem.*, **42**, 30 (2007).
[10] B.K. Park, N.R. Kitteringham, P.M. O'Neill. *Annu. Rev. Pharmacol. Toxicol.*, **41**, 443 (2001).
[11] R.F. Heck, J.P. Nolley. *J. Org. Chem.*, **37**, 2320 (1972).
[12] V. Polshettiear, C. Len, A. Fihri. *Coord. Chem. Rev.*, **253**, 2599 (2009).
[13] S.M. Isiam, P. Mondal, K. Tuhina, A.S. Roy, S. Mondal, D. Hossain. *J. Inorg. Organomet. Polym.*, **20**, 264 (2010).
[14] Bruker. APEXII Software, Version 6.3.1, Bruker AXS Inc, Madison, WI (2004).
[15] S. Parkin, B. Moezzi, H. Hope. *J. Appl. Cryst.*, **28**, 53 (1995).
[16] G.M. Sheldrick. *Acta Cryst.*, **A64**, 112 (2008).
[17] Y. Fuchita, K. Yoshinaga, T. Hanaki, H. Kawano, J. Kinoshita-Nagaoka. *J. Organomet. Chem.*, **580**, 273 (1999).
[18] A. Crispini, G.D. Munno, M. Ghedini, F. Neve. *J. Organmet. Chem.*, **427**, 409 (1999).
[19] L. Paluling. *The Nature of Chemical Bond*, Cornell University Press, New York, NY (1960).
[20] G. Zhao, Q.G. Wang, T.C. Mak. *Polyhedron*, **18**, 577 (1999).
[21] C.K. Jørgensen. *Prog. Inorg. Chem.*, **12**, 101 (1970).

[22] A.B.P. Lever. *Inorganic Electronic Spectroscopy*, 2nd Edn, Elsevier, Amsterdam (1984).
[23] D.A. Roberts, W.R. Mason, G.L. Geoffroy. *Inorg. Chem.*, **20**, 789 (1981).
[24] J.M. Dawson, T.J. McLennan, W. Robinson, A. Merle, M. Dartiguenave, Y. Dartiguenave, H.B. Gray. *J. Am. Chem. Soc.*, **96**, 4428 (1974).
[25] C.B. Pamplin, S.J. Rettig, B.O. Patrick, B.R. James. *Inorg. Chem.*, **42**, 4117 (2003).
[26] X.X. Lu, E.C.C. Cheng, N. Zhu, V.W.W. Yam. *Dalton Trans.*, 1803 (2006).
[27] O.E. Offiong, E. Nfor, A.A. Ayi. *Transition Met. Chem.*, **25**, 369 (2000).
[28] M.A. Carvalho, B.C. Souza, R.E.F. Paiva, F.R.G. Bergamini, A.F. Gomes, F.C. Gozzo, W.R. Lustri, A.L.B. Formiga, G. Rigatto, P.P. Corbi. *J. Coord. Chem.*, **65**, 1700 (2012).
[29] A.A. El-Sherif. *J. Coord. Chem.*, **64**, 2035 (2011).
[30] A.C. Moro, A.C. Urbaczek, E.T. De Almeida, F.R. Pavan, C.Q.F. Leite, A.V.G. Netto, A.E. Mauro. *J. Coord. Chem.*, **65**, 1434 (2012).
[31] M.N. Patel, P.A. Dosi, B.S. Bhatt. *J. Coord. Chem.*, **65**, 3833 (2012).
[32] N.T. Abdel-Ghani, A.M. Mansour. *J. Coord. Chem.*, **65**, 763 (2012).
[33] M.K. Biyala, K. Sharma, M. Swami, N. Fahmi, R.V. Singh. *Transition Met. Chem.*, **33**, 377 (2008).